AFRL-OSR-VA-TR-2014-0088

SOLAR TO LIQUID FUELS PRODUCTION: LIGHT-DRIVEN REDUCTION OF CARBON DIOXIDE TO FORMIC ACID

John Golbeck
PENNSYLVANIA STATE UNIVERSITY

04/02/2014
Final Report

Air Force Research Laboratory
AF Office Of Scientific Research (AFOSR)/ RTE
Arlington, Virginia 22203
Air Force Materiel Command

REPORT DOCUMENTATION PAGE

Form Approved
OMB No. 0704-0188

1. REPORT DATE *(DD-MM-YYYY)*	**2. REPORT TYPE**	**3. DATES COVERED** *(From - To)*
29-03-2014	final	15-09-2009 to 31-12-2013

4. TITLE AND SUBTITLE

Solar to Liquid Fuels Production: Light-Driven Reduction of Carbon Dioxide to Formic Acid

5a. CONTRACT NUMBER

5b. GRANT NUMBER
FA9550-09-1-0671

5c. PROGRAM ELEMENT NUMBER

6. AUTHOR(S)
Golbeck, John H.
Bryant, Donald A
Lubner, Carolyn E.
Gorka, Michael
Applegate, Amanda

5d. PROJECT NUMBER

5e. TASK NUMBER

5f. WORK UNIT NUMBER

7. PERFORMING ORGANIZATION NAME(S) AND ADDRESS(ES)
The Pennsylvania State University
Office of Sponsored Programs
110 Technology Center
University Park, PA 16802

8. PERFORMING ORGANIZATION REPORT NUMBER

9. SPONSORING / MONITORING AGENCY NAME(S) AND ADDRESS(ES)
Air Force Office of Scientific Research
AFOSR/NL
875 North Randolph Street
Suite 325, Room 3112

10. SPONSOR/MONITOR'S ACRONYM(S)

11. SPONSOR/MONITOR'S REPORT NUMBER(S)

12. DISTRIBUTION / AVAILABILITY STATEMENT

Public Availability

13. SUPPLEMENTARY NOTES

14. ABSTRACT

Project FA9550-09-1-0671 involved generating formic acid from CO2 using sunlight as the source of energy. The method chosen was to engineer a Photosystem I-molecular wire-formic acid dehydrogenase (FDH) bioconjugate that would carry out the half-cell reaction CO2 + 2e– + 2H+ + 2hv → H2CO2. The work had three specific goals: (Aim 1) to generate a Cys → Gly variant of the Escherichia coli FDH enzyme to provide a point of attachment for a molecular wire; (Aim 2) to modify Photosystem I (PS I) from Synehocystis sp. PCC 6803 so that electrons can be withdrawn from a point in the electron transfer chain that would provide the requisite redox potential for CO2 reduction at atmospheric concentrations; and (Aim 3) to construct a PS I-molecular wire-FDH bioconjugate that would function as a direct light-driven CO2 to formic acid photo-electrochemical half-cell. Aim 1 was successful in that a catalytically-active C42G variant of FdhF was generated that contained a cysteine rather than a selenocysteine (U140C). Aim 2 was also successful in that a naphthoquinone-containing molecular wire consisting could be introduced into the A1A and A1B sites of the menB variant of PS I and could transfer 134 electrons mg Chl-1 h-1 to an external catalyst in the light. Aim 3 was partiall

15. SUBJECT TERMS

16. SECURITY CLASSIFICATION OF:			**17. LIMITATION OF ABSTRACT**	**18. NUMBER OF PAGES**	**19a. NAME OF RESPONSIBLE PERSON**
					John H. Golbeck
a. REPORT	**b. ABSTRACT**	**c. THIS PAGE**	UU	1	**19b. TELEPHONE NUMBER** *(include area code)*
U	U	U			1 814 865 1163

Project FA9550-09-1-0671: Solar to Liquid Fuels Production: Light-Driven Reduction of Carbon Dioxide to Formic Acid

Project FA9550-09-1-0671 was funded to generate formic acid from CO_2 using sunlight as the source of energy. The method chosen was to engineer a Photosystem I-molecular wire-formic acid dehydrogenase (FDH) bioconjugate that would carry out the half-cell reaction $CO_2 + 2e^- + 2H^+ + 2h\nu \rightarrow H_2CO_2$. The work had three specific aims: (i) to generate a Cys → Gly variant of the *Escherichia coli* FDH enzyme to provide a point of attachment for a molecular wire; (ii) to modify Photosystem I (PS I) so that electrons can be withdrawn from a point in the electron transfer chain that would provide the requisite redox potential for CO_2 reduction at atmospheric concentrations; and (iii) to construct a PS I-molecular wire-FDH bioconjugate that would function as a direct light-driven CO_2 to formic acid photo-electrochemical half-cell. The formic acid produced is a portable, liquid fuel, and can be used to generate electricity in a direct formic acid fuel cell. Recent developments in polymer electrolyte membrane fuel cell technology have made formic acid an attractive alternative to methanol (which requires a more complicated 6-electron reduction of CO_2) or methane (an even more complicated 8-electron reduction of CO_2). A direct formic acid fuel cell can operate under ambient air and at zero back pressure at 18° C to 70° C and it can achieve power densities in excess of 250 mW/cm^2. Even though neat formic acid has less than one-half the energy density of neat methanol (2086 Wh/l vs 4609 Wh/l), a direct formic acid fuel cell can be fed with a higher concentration of feedstock. However, the reduction of CO_2 to formic acid is mechanistically difficult, and at this time, is best achieved by using enzymes. The work funded by the AFOSR was to engineer a biohybrid device that contains a light-driven component (Photosystem I), a catalyst (formic acid dehydrogenase) and a linker to tether the two proteins. Progress in achieving this goal is described below.

Aim 1: Engineering the Cys → Gly variant of formic acid dehydrogenase

Similar to the evolution of the hydrogenase enzyme, which reduces protons to H_2, a class of enzymes termed formic acid dehydrogenases has evolved that can reduce CO_2 to formic acid. The reaction can be summarized as:

$$CO_2 + 2H^+ + 2e^- \rightarrow H_2CO_2$$

Electrochemical studies have shown that FDH begins to reduce CO_2 to formic acid at approximately –0.4 V (1), which is close to its standard thermodynamic midpoint potential of –0.389 V. As the potential is decreased, the rate of formic acid production increases linearly up to a maximum of –0.8 V. CO_2 reduction is greatest at pH 5.5, but it occurs, albeit at lower rates, at pH 7.0 and then tapers off, becoming negligible around pH 8. When the enzyme is studied in solution with benzyl viologen as the electron donor, the turnover rate is 282 s^{-1}, which is equivalent to 564 electrons s^{-1}. This is an electron throughput that can readily be supplied by cyanobacterial Photosystem I (PS I), which has a turnover number of ~1000 electrons s^{-1} in full sunlight. To exploit the electron throughput of PS I for light driven formic acid production, it is necessary to connect the iron-sulfur clusters of the two enzymes with the use of a molecular wire. The X-ray crystal structure for the *E. coli* FDH enzyme shows that a [4Fe-4S] cluster is located near the surface of the protein. The first goal of this research project is to change a surface located Cys residue to Gly. This provides an open coordination site of the [4Fe-4S]

cluster, making it accessible to a thiol-containing rescue ligand. If the rescue ligand were attached to PS I in the form of a molecular wire, it should be possible to transfer electrons from PS I to FDH at sufficiently low reduction potentials and high rates to affect the reduction of atmospheric CO_2 to formic acid. *E. coli* FDH, encoded by *fdhF*, was chosen for this work because it is a single-subunit enzyme that has been studied in detail, and for which a crystal structure exists (2). The active site of this enzyme contains a molybdenum atom coordinated by two pterin cofactors and a selenocysteine residue, and a single [4Fe-4S] cluster through which electrons are transferred. The [4Fe-4S] cluster is surface-exposed and ligated to the N-terminal domain of the protein by a CPYCASGC//C motif (3), which includes Cys residues 8, 11, 15, and 42. Oligonucleotide-directed, site-specific mutagenesis was employed to change surface-located Cys_{11} to Gly to open a coordination site. The proteins were overproduced in *E. coli* and purified for further characterization as described below.

Designing an expression construct for FdhF *production*

Both the gene encoding wild-type *E. coli* FDH, *fdhF*, and the gene encoding the selenocysteinyl-tRNA, *selC*, were cloned into pCOLADuet, under the control of the T7 promoter, for expression in BL21(DE3). In this construct, FdhF has an N-terminal 6X-His tag to facilitate purification. However, no detectable protein was produced as visualized by whole cell Western blotting with an anti-his antibody. Pinske, et al. (4) suggested that BL21-derived strains have deficiencies in molybdenum transport, hence, constructs were instead expressed in *E. coli* strains MC1061 and MC4100, which are not known to have problems with molybdenum transport. At this time, we also received a construct from Silke Leimkuhler (University of Potsdam, Germany) containing a selenocysteine to cysteine (U140C) variant FdhF expressed from pTrc99a in the *E. coli* strain MC1061. *E. coli* FdhF has been shown to retain around 5 to 10% activity when the selenocysteine residue is replaced with cysteine (5). From this point forward, our efforts were split between two approaches: *Approach 1* would utilize *E. coli* strain MC1061 with a selenocysteine to cysteine mutation (U140C) in FdhF, and *Approach 2* would utilize *E. coli* strain MC4100 with the selenocysteine residue conserved in FdhF. A C42G mutation, which should allow molecular wire accessibility to the [4Fe-4S] cluster, was employed in both approaches, as well as the expression of *fdhF* from pTrc99a.

Expression studies were carried out to select for a construct that would produce the most protein. In many cases, a band appeared on an SDS-PAGE gel at the appropriate molecular weight for FdhF. It was determined that this was probably native FdhF enzyme, as this band did not always translate into a band in Western blots against anti-his antibody. We hypothesized that when native FdhF is present, the variants may be more rapidly targeted for degradation. Accordingly, the chromosomal copies of both *fdhF* and the recombinase, *recA*, were deleted to prevent recombination of variant constructs with the wild-type. This also ensured that the cofactors are incorporated only into the plasmid-encoded variant FdhF, thereby allowing the cell to put more energy into making the variant enzyme. Deletion of the native *fdhF* did result in a band at the correct molecular weight on an SDS-PAGE that was also visualized in anti-his Western blots for both the MC1061 and MC4100 constructs.

We noted that the N-terminal 6X-His tag was close to the cysteine residues that coordinate the [4Fe-4S] cluster. Because purification of the enzyme was performed by affinity chromatography, having a his-tag in close proximity to this cofactor may have resulted in degradation of the iron-sulfur cluster and thus a decrease in activity. We observed several his-tagged degradation products after purification, confirming this hypothesis, and we therefore moved the 6X-His tag to the C-terminus, away from the cofactor binding site. C-terminally tagged FdhF resulted in fewer degradation products during purification, as well as improved expression of the FdhF variants (**Figure 1**).

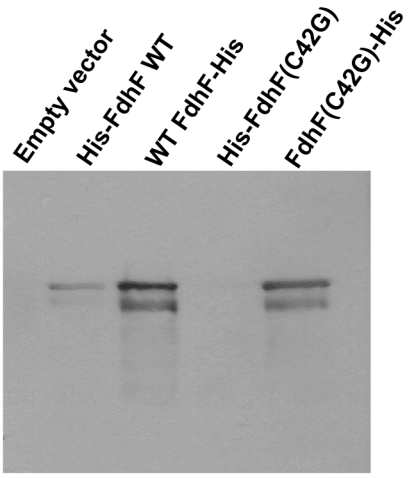

Figure 1. Western blot against the 6X-His tag for cultures expressing N-terminally His-tagged FdhF (lanes 2 and 4), or C-terminally His-tagged FdhF (lanes 3 and 5).

Akhtar, et al. (6), showed that deletion of the transcriptional repressor *iscR* from *E. coli* results in higher yield and higher specific activity of heterologously-expressed iron-sulfur cluster containing proteins. We received the Δ*iscR* allele from Patricia Kiley (U. of Wisconsin) and moved this allele into both the cysteine and selenocysteine FDH constructs. We observed a high yield of cells and active protein expressed in this strain for the MC1061 constructs (*Approach 1*). This has not yet been investigated for the MC4100 constructs (*Approach 2*).

Optimization of Expression Conditions

Approach 1: Cysteine-containing FdhF

Cysteine-containing FdhF is only 5 to 10% as active as selenocysteine-containing FdhF. However, due to the complicated nature of selenocysteine incorporation into proteins, the cysteine-containing FdhF construct was expected to produce viable enzyme more readily and, thus, we focused most of our work on this approach.

A number of parameters were studied such as growth temperature, amount of oxygen and aeration in the media, induction method, medium composition, and supplements present. The optimization was performed on the MC1061 Δ*fdhF* strain with the C-terminally his-tagged FdhF (either U140C single mutant or U140C/C42G double mutant). It was found that during growth in LB media, both the single and double mutants optimally expressed FdhF at 30 °C rather than 37 °C, although more biomass was produced at the higher temperature. These cultures were supplemented with 150 μg/mL ampicillin, 1 mM sodium molybdate, and induced with a constant, low level of IPTG (20 μM added at inoculation). They were grown either with full aeration (aerobic), minimal aeration as defined by standing cultures with minimal aeration but not completely purged of oxygen (semi-anaerobic), or shaking but fully purged of oxygen (anaerobic). Semi-anaerobic conditions resulted in the highest expression of enzyme (for both temperatures). No significant increase in FdhF expression was observed when the induction method was changed (0.5 mM IPTG when cell density reached an OD600 = 0.6). It should be

noted that the overall biomass yield was very small, and we attempted large-scale growth in 60-liter bioreactors to obtain useful quantities of enzyme. However, based on the low yield of enzyme produced and the relative inactivity found with these growth methods, it is likely that the cell was unable to insert all of the cofactors into FdhF under the chosen growth conditions. Indeed, the purified protein had a featureless absorption spectrum consistent with lack of the iron-sulfur cluster.

To increase the FdhF-containing plasmid yield, as well as to extend the growth phase of our recombinant *E. coli*, the enriched medium, 'Terrific Broth' (TB), was employed. When the same constructs were expressed in TB medium containing the same supplements as described above (150 μg/mL ampicillin, 1 mM sodium molybdate, and 20 μM IPTG), an increase in cell mass was realized. The washed cells were brown in color, which is typical of *E. coli* cells expressing iron-sulfur cluster-containing proteins. FdhF purified from these cells showed a characteristic Fe/S charge transfer band at 420 nm that decreased in amplitude when reduced with sodium dithionite. In addition, the purified FdhF was found to be functionally active.

Further optimization of the growth conditions involved the use of a spinner flask, which allows for control of atmospheric conditions while providing agitation to the cell culture. In this setup, the culture was allowed to grow under optimal conditions for *E. coli* (37 °C with full aeration) until late log phase, at which point the culture was induced with 0.5 mM IPTG and 1 mM L-cysteine, and purged with Ar gas to ensure anaerobicity. Additional supplements were also added (2 mM ferric ammonium citrate at inoculation) to facilitate iron-sulfur cluster insertion. The culture was allowed to grow overnight (<25 hours total growth time) at room temperature (25 °C) with continuous Ar purging. This method resulted in a 10-fold improvement of yield (~6 g/L), and produced very dark brown colored cells. When the *iscR* deletion was added to this strain and grown following this method, a further improvement in cell yield (~10 g/L) was realized. When the double mutant of this strain was grown and crudely purified, FdhF at the correct molecular weight was visualized on Western blots against an anti-his antibody in high yields (**Figure 2**).

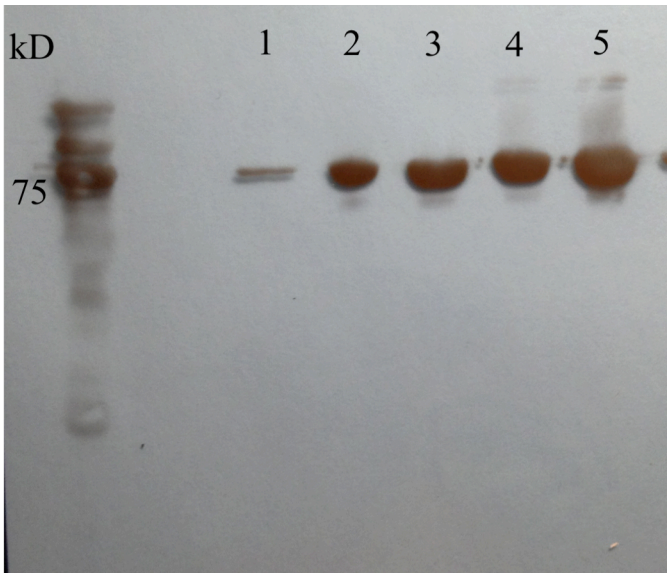

Figure 2. Western blot against the 6X-his tag on whole cells of MC1061 Δ*fdhF* Δ*iscR* U140C C42G C-terminal his FdhF grown under optimal conditions (1) and elution fractions after anaerobic affinity column purification (2-5).

Purification and Activity Assays

Purification of cysteine-containing FdhF was performed under anaerobic conditions to preserve the activity of the enzyme. At first, lysis was carried out on the bench under argon gas, but subsequently lysis was performed under a strict anaerobic atmosphere. Purification conditions were attempted with various buffers (50 mM Tris, pH 8.3, 50 mM potassium phosphate pH 7.6, 100 mM MOPS, pH 7) and salts (sodium chloride, sodium gluconate), however due to the low activity of the enzyme, it was difficult to correlate purification conditions with activity in the crude lysates.

FdhF was eventually purified from the brown fractions at high purity and yield. The purified FdhF shows a typical absorption spectrum for an iron-sulfur cluster-containing protein. Activity assays were carried out using a benzyl viologen linked reaction scheme in which oxidized benzyl viologen (as colorimetric indicator) and formic acid (as substrate) are added to the FdhF enzyme. On catalysis, benzyl viologen accepts the electrons from the oxidation of formic acid and the reaction is visualized by an absorbance change at 600 nm. The U140C/C42G FdhF variant was shown to support a rate of 74 electrons $FdhF^{-1}$ min^{-1}. Benzyl viologen reduction was only observed for fractions containing FdhF. Some FdhF enzymes have the ability to perform redox chemistry with the NADP+/NADPH couple (7). Two assays were designed for which NADP+/NADPH act as the electron acceptor/donor, in the presence of formic acid or bicarbonate, as respective substrates, and the NADP+/NADPH redox activity was monitored at 340 nm. However, our FdhF enzyme does not appear to have the ability to interact with NADP+/NADPH. FdhF activity will therefore be measured through the formic acid oxidation assay until we develop an appropriate assay for formic acid generation. Nevertheless, this work showed that we were able to generate large amounts of a cysteine-containing variant FdhF that had low, but measurable, activity.

Approach 2: Selenocysteine-containing FdhF

We expect selenocysteine-FdhF to have considerably higher activity than its cysteine-containing counterpart, and therefore have tried to optimize expression of this protein as well. This approach additionally included the co-expression of genes to aid in the incorporation of the selenocysteine residue. Selenocysteine is encoded by an amber stop codon, making incorporation of this non-canonical amino acid into heterologously expressed proteins potentially difficult. Initially, *selC* was cloned separately into pSU21, under the control of P_{Lac}, and co-expressed with *fdhF* in *E. coli* strain MC4100. We also tried cloning the genes for selenocysteine synthase (*selA*) and the selenocysteinyl-tRNA elongation factor

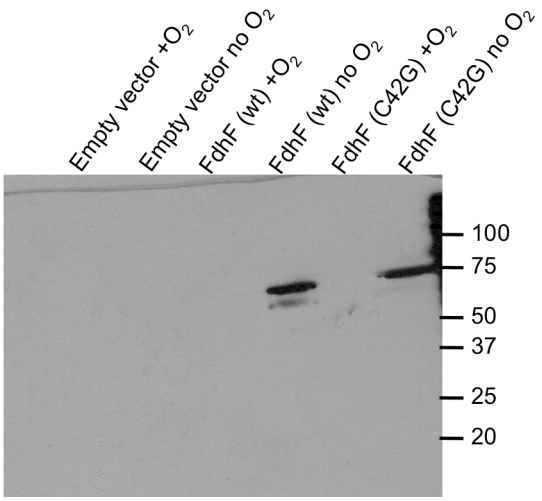

Figure 3. Western blot on cell lysates from cultures grown under aerobic (Lanes 1, 3, 5) or anaerobic (Lanes 2, 4, 6) conditions.

(*selB*) into pMQ132, also under the control of a lac promoter. However, co-expressing *selAB* with *fdhF* and *selC* did not seem to enhance expression of the selenocysteine-containing FdhF.

The MC4100Δ*fdhF*Δ*recA* pTrc99a-*fdhF* pSU21-*selC* strain was grown in LB media supplemented with 100 μg/mL ampicillin, 20 μg/mL chloramphenicol, 10 μM sodium selenite and 1 mM sodium molybdate. Expression of the selenocysteine-containing FdhF was higher in cultures grown at 30 °C compared to 37 °C, and expression of this protein required anaerobic growth (**Figure 3**). Based on results from the expression of cysteine-containing FdhF, outlined above, we expressed selenocysteine-containing FdhF in a similar manner, *i.e.* in a spinner flask in Terrific Broth, supplementing with not only molybdenum and selenium, but also L-cysteine and ferric ammonium citrate to maximize incorporation of the essential cofactors. However, the yields of the selenocysteine FDH enzyme were extremely low, and we were unable to purify enough to detect activity.

To conclude, we were successful in generating a C42G variant of FdhF that contained a cysteine rather than a selenocysteine that could be used for tethering to Photosystem I (see Aim 3 below).

Aim 2: Modifying PS I so that electrons can be withdrawn from the A_{1A}/A_{1B} sites

Electron transfer from the terminal F_B cluster of PS I to the Mo catalytic center of FDH is thermodynamically favorable by –160 mV, which translates to an equilibrium constant of ~500 in favor of formic acid production. However, this value is only valid under standard biochemical conditions, which is 1 M of product and reactant in solution, and 1 atm of gas. The current concentration of carbon dioxide in the atmosphere is ~400 ppm, which when corrected for by the Nernst equation, would require a potential of ~ –650 mV. Additionally, electrochemical studies carried out on the *Syntrophobacter fumaroxidans* formic acid dehydrogenase enzyme indicate that the rate of formic acid production increases as the driving force increases from –0.40 V to –0.80 V (1). It would therefore be highly desirable to attain the largest possible driving force between PS I and FDH. Because there is very little latitude to alter the midpoint potentials of the F_A or F_B iron-sulfur clusters, a larger driving force can be achieved by capturing the electron earlier in the electron transfer chain of PS I, either at F_X or at A_{1A}/A_{1B}.

Steric constraints imposed by the PsaA/PsaB heterodimer make it difficult to devise a method to attach a molecular wire to the F_X cluster. However, a variety of techniques exist to introduce alternative quinones into the A_{1A} and A_{1B} sites. Solvent extraction with wet diethyl ether or hexane/methanol removes the majority of the chlorophylls and most, if not all, of the quinones and carotenoids. However, it leaves the six core chlorophylls intact that are involved in charge separation (P_{700}, A_{-1A}/A_{1B} and A_{0A}/A_{0B}) as well as the F_X, F_A and F_B clusters. A wide range of naphthoquinones to be incorporated into the empty A_{1A} and A_{1B} binding sites. This method was exploited by Terasaki et al. (8), who introduced the substituted naphthoquinone, $NQ(CH_2)_{15}S$-Au into the A_{1A} and A_{1B} sites to fabricate a bio-photosensor. We exploited this method to determine whether electrons can be extracted from the A_{1A}/A_{1B} sites at sufficiently high rates to carry out catalysis. We did this by synthesizing 1-4-(1,4-dihydro-3-methyl-1,4-dioxonaphthalen-2-yl)butyl]-4,4'-bipyridinium disulfide (abbreviated $(NQ(CH_2)_4BP(CH_2)_4S)_2$), which contains a naphthoquinone connected to a 4,4'-bipyridinium dye through a four carbon methylene spacer. Because bipyridinium shows a strong absorption at 600 nm when singly reduced, the rate of

electron transfer can be followed by optical absorption spectroscopy. $NQ(CH_2)_4BP(CH_2)_4S)_2$ was reduced to the free thiol, and acetylated to produce $NQ(CH_2)_4BP(CH_2)_4SAc$. When added to solvent-extracted PS I, long-lived charge recombination was restored, indicating that the naphthoquinone group had indeed occupied the A_{1A}/A_{1B} sites. When the construct was illuminated, a linear increase in absorbance at 600 nm was observed for ~20 min, and the rate of electron transfer to the 4,4'-bipyridinium was calculated to be 47.2 ± 1.49 μmole • mg Chl^{-1} • h^{-1}, which is similar to the rate of 53.3 μmole • mg Chl^{-1} • h^{-1} when a 4,4'-bipyridinium is tethered to the F_B site through 1,6-hexanedithiol under similar experimental conditions (9). These values are similar because of a common donor side limitation on the rate of P_{700}^+ reduction by the soluble cytochrome c_6 donor. This experiment gave us confidence that the electron could be extracted from the A_{1A}/A_{1B} sites and that it could support high rates of light-driven catalysis.

A genetic method to introduce alternative quinones into PS I is also available, which involves interruption of the *menA*, *menB*, *menD,* or *menE* genes (10-14). With any of these genes inactivated, the biosynthesis of phylloquinone is blocked, and plastoquinone-9 occupies the A_{1A} and A_{1B} sites. Plastoquinone-9 is loosely bound and can be displaced with a variety of substituted naphthoquinones. This method of quinone exchange has the advantage over solvent extraction that all of the chlorophylls and carotenoids are retained in the PS I complexes. However, the FDH variant was not available when Aim 2 was being developed, hence we used a Pt nanoparticle and hydrogen evolution as a proxy. The experiment was to determine whether a construct based on Pt generates hydrogen under illumination and whether the transfer of the electrons from the A_{1A} and A_{1B} sites occurs during the forward reaction or the back reaction. On one hand, the alkyl chain must be long enough to span the distance between the A_1 site(s) and the surface of the protein because the Pt nanoparticle is not able to penetrate into the hydrophobic core. On the other hand, the rate of electron transfer between the quinone and the nanoparticle decreases exponentially as the length of the tether increases. Thus, there should be an optimal length for the tether corresponding to the minimum distance between the A_1 site and the protein surface. Based on the X-ray crystal structure of PS I, we estimated this distance to be on the order of half the trans-membrane distance of 30 Å. The length of the alkyl tether depends on its conformation but the maximum length of a 15 carbon alkyl chain is roughly 22.5 Å. Hence, a construct with a 15 carbon chain was deemed to be sufficient to span the required distance. We synthesized a series of quinone molecules, including 1-[10-(3-methyl-1,4-naphthoquinone-2-yl)]decyl disulfide and 1-[15-(3-methyl-1,4-naphthoquinone-2-yl)]pentadecyl disulfide. These modified naphtho-quinones were added to the *menB* variant of PS I; the naphthoquinone head group displaced the plastoquinone-9, as expected, allowing it to function as an electron transfer cofactor. The disulfide was then reduced to a free sulfhydryl, a Pt nanoparticle was attached to the thiol, and the rate of hydrogen evolution was measured under illumination.

The resulting PS I–$NQ(CH_2)_{15}S$–Pt nanoconstruct evolved hydrogen at a rate of 67.3 μmol H_2 mg Chl^{-1} h^{-1} (3.4 e^- PS I^{-1} s^{-1}) at pH 6.4. No hydrogen was detected if wild-type PS I was used, which does not incorporate the quinone, or if either $(NQ(CH_2)_{15}S)_2$ or the Pt nanoparticle was absent. Time-resolved optical studies of the PS I–$NQ(CH_2)_{15}S$–Pt nanoconstruct showed that the lifetimes of the forward and reverse electron transfer to and from the iron-sulfur clusters were identical to native PS I. Thus, electrons are not transferred directly from the quinone to the Pt nanoparticle during either forward or reverse electron transfer. Most importantly, it was found

that the rate of hydrogen evolution in the PS I–NQ$(CH_2)_{15}$S–Pt nanoconstruct depends strongly on the concentration of the sacrificial electron donor cytochrome c_6.

We proposed a mechanism, shown in **Figure 4**, to account for the lack of hydrogen evolution at low concentrations of cytochrome c_6. The ability of the electron to be transferred through the molecular wire to the Pt nanoparticle is a function of the forward rate constant, k_2, relative to forward electron transfer to the iron-sulfur clusters (simplified here as a single rate constant, k_1) and the charge recombination channel, k_r. Because the electronic coupling decreases exponentially with the distance and because a significant activation energy is expected, under nearly all reasonable configurations of the molecular wire-Pt nanoparticle adduct, k_2, will be much smaller than k_1, hence the electron will have only a small probability of being transferred to the Pt nanoparticle during forward electron transfer. The value of k_2 also needs to be considered in relation to k_{-2}, and k_r. The relative magnitude of k_2 and k_r can be estimated from the kinetics of electron transfer in PS I in the absence of the iron-sulfur clusters. Here, the electron on either A_{1A} or A_{1B} has only two available routes: it can either recombine with P_{700}^+ with rate constant k_r or it can be transferred to the Pt nanoparticle with rate constant k_2. The fate of the electron will be determined by the relative values of k_2 and k_r. While the value of k_2 is not known, the large distance between the naphthoquinone head group and the Pt nanoparticle as well as the presence of σ-bonds throughout the hydrocarbon tether will most certainly render k_2 much less than k_r. Finally, the relative values of k_2 and k_{-2} need to be considered. The ratio k_2/k_{-2} is given by $k_2/k_{-2} = \exp(-\Delta G/kT)$, using an estimate for ΔG of –241 mV for the A-branch and –414 mV for the B-branch we get a k_2/k_{-2} ratio of 10^4 (A-branch) or 10^7 (B-branch). Because k_2 is much smaller than k_r and k_1, electron transfer to the Pt nanoparticle can only occur if charge recombination is inhibited. Because k_{-2} is negligible, the electrons become trapped. The rate of trapping is given by $k_{-1}\, k_2/k_1$. These rate constants are not known accurately but k_1 is on the order of 10^7 s^{-1}. In the absence of the iron sulfur clusters, the charge recombination from A_{1A}^- occurs with a lifetime of 95 μs, so $k_r \approx 10^4$ s^{-1}. Using these two values, the observed 65 ms lifetime for the back reaction from F_B in native PS I yields $k_{-1} \approx 1.6\times10^4$ s^{-1}. If we assume that k_2 is an order of magnitude smaller than k_r, we obtain a rate of ~1 s^{-1} for the trapping of electrons on the Pt nanoparticle. When two electrons are serially transferred to the Pt nanoparticle, the release of hydrogen makes electron transfer irreversible.

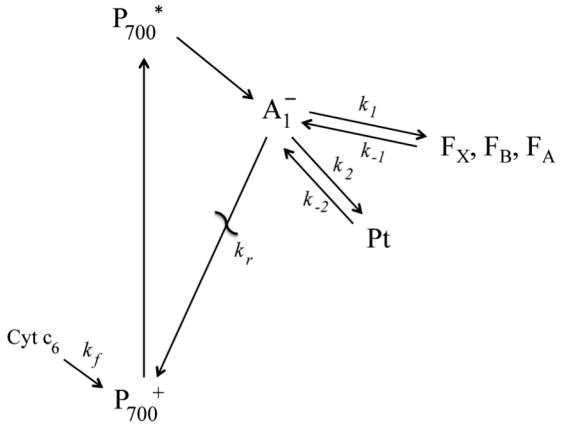

Figure 4. The kinetic routes available for an electron residing on A_1.

These observations show that the iron-sulfur clusters are involved in stabilizing the electron; the ~65 ms residence time of the electron on F_A/F_B is sufficiently long to allow cytochrome c_6 to reduce P_{700}^+, thereby eliminating the recombination channel. In the absence of P_{700}^+, slow electron transfer through the molecular wire to the Pt catalyst can occur and hence H_2 evolution is observed.

To conclude, we were successful in introducing a naphthoquinone-containing molecular wire into the A_{1A} and A_{1B} sites of the *menB* variant of PS I and in transferring an electron to a catalyst.

Aim 3: Construction of the PS I-molecular wire-FDH bioconjugate

We constructed the PS I-molecular wire-FDH bioconjugate by tethering the U140C/C42G FdhF variant enzyme to the F_B cluster rather than to the A_{1A}/A_{1B} sites (**Figure 5**). We did this for two reasons. First, the techniques for introducing a naphthoquinone-containing molecular wire into the A_{1A} and A_{1B} sites of the *menB* variant of PS I (Aim 2) were still under development. Second, our earlier work on hydrogen production involved tethering a [FeFe]-hydrogenase to the F_B cluster, and this allowed the rates of hydrogen and formic acid production to be directly compared. PS I and U140C/C42G FdhF were connected in a 1:1 ratio using 1,8-octanedithiol as a linker, and allowed to assemble for 1 hour under anaerobic conditions in the dark. The sample was illuminated for 15 minutes in the presence of 100 mM bicarbonate and assayed in the dark for formic acid. This assay employed an oxygen stable FDH enzyme, which favors formic acid oxidation, coupled to the reduction of NAD+ to form NADH. From previous experiments described in Aim 2, we knew that our variant FdhF enzyme does not interact with NAD+/NADH or NADP+/NADPH, thereby ensuring there are no side reactions between our wired FdhF and the NAD+ reporter. The absorbance change at 340 nm (NADH) was measured and a small, but reproducible change was observed, corresponding to a rate of formic acid production of 35 µmol mg Chl^{-1} hr^{-1}. (A [FeFe]-hydrogenase attached to the F_B cluster generates hydrogen at a rate of 2200 µmol H_2 mg Chl^{-1} h^{-1} (15)). This rate of formic acid production corresponds to an electron throughput of 100 e^- PS I^{-1} min^{-1}, and is therefore similar to the observed variant FdhF activity (74 e^- $FdhF^{-1}$ min^{-1}). Preliminary control experiments confirmed that no formic acid was produced when the sample was not illuminated or when FdhF was not present. The generation of formic acid still needs to be confirmed using a more direct HPLC-based assay, and additional variables need to be studied, especially buffer strength, pH, and substrate concentration, in future experiments.

To conclude, we have evidence that the PS I-molecular wire-FDH bioconjugate attached to the F_B site generates formic acid from carbon dioxide in the light. It is expected that extraction of the electron at the A_{1A}/A_{1B} sites site of PS I should increase the driving force, and thus the rate, of formic acid production.

Because of the termination of the AFOSR biofuels program, confirmation of this result, as well as extension of this technology to include the tethering of the U140C/C42G FDH enzyme to the A_{1A}/A_{1B} sites, will need to be carried out with funding from another agency.

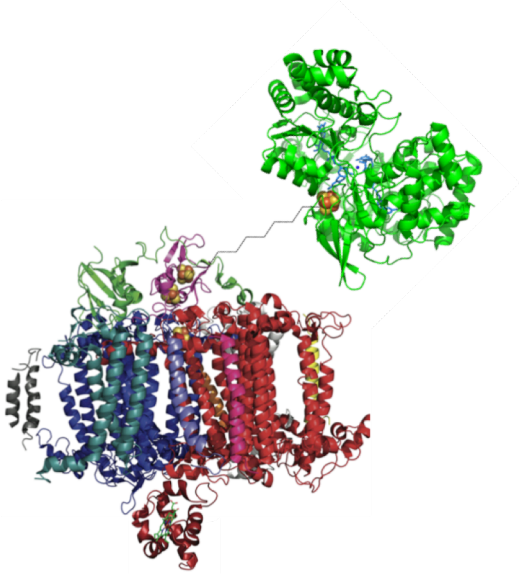

Figure 5. Schematic of the PS I-molecular wire-FdhF bioconjugate using 1,8-octanedithiol to link the modified [4Fe-4S] clusters in each protein.

References

1. Reda, T., Plugge, C. M., Abram, N. J., and Hirst, J. (2008) Reversible interconversion of carbon dioxide and formate by an electroactive enzyme. *Proc Natl Acad Sci U S A* **105**, 10654-10658
2. Boyington, J. C., Gladyshev, V. N., Khangulov, S. V., Stadtman, T. C., and Sun, P. D. (1997) Crystal structure of formate dehydrogenase H: catalysis involving Mo, molybdopterin, selenocysteine, and an Fe4S4 cluster. *Science* **275**, 1305-1308
3. Gladyshev, V. N., Boyington, J. C., Khangulov, S. V., Grahame, D. A., Stadtman, T. C., and Sun, P. D. (1996) Characterization of crystalline formate dehydrogenase H from Escherichia coli. Stabilization, EPR spectroscopy, and preliminary crystallographic analysis. *J Biol Chem* **271**, 8095-8100
4. Pinske, C., Bonn, M., Kruger, S., Lindenstrauss, U., and Sawers, R. G. (2011) Metabolic deficiences revealed in the biotechnologically important model bacterium Escherichia coli BL21(DE3). *PLoS One* **6**, e22830
5. Axley, M. J., Bock, A., and Stadtman, T. C. (1991) Catalytic properties of an Escherichia coli formate dehydrogenase mutant in which sulfur replaces selenium. *Proc Natl Acad Sci U S A* **88**, 8450-8454
6. Akhtar, M. K., and Jones, P. R. (2008) Deletion of iscR stimulates recombinant clostridial Fe-Fe hydrogenase activity and H2-accumulation in Escherichia coli BL21(DE3). *Appl Microbiol Biotechnol* **78**, 853-862
7. Alissandratos, A., Kim, H.-K., Matthews, H., Hennessy, J. E., Philbrook, A., and Easton, C. J. (2013) Clostridium carboxidivorans Strain P7T Recombinant Formate Dehydrogenase Catalyzes Reduction of CO2 to Formate. *Applied and Environmental Microbiology* **79**, 741-744
8. Terasaki, N., Yamamoto, N., Tamada, K., Hattori, M., Hiraga, T., Tohri, A., Sato, I., Iwai, M., Iwai, M., Taguchi, S., Enami, I., Inoue, Y., Yamanoi, Y., Yonezawa, T., Mizuno, K., Murata, M., Nishihara, H., Yoneyama, S., Minakata, M., Ohmori, T., Sakai, M., and Fujii, M. (2007) Bio-photosensor: Cyanobacterial photosystem I coupled with transistor via molecular wire. *Biochim Biophys Acta* **1767**, 653-659
9. Lubner, C., Heinnickel, M., Bryant, D. A., and Golbeck, J. H. (2011) Wiring Photosystem I for Electron Transfer to a Tethered Redox Dye. *Energy Environ Sci* **4**, 2428-2434
10. Johnson, T. W., Shen, G., Zybailov, B., Kolling, D., Reategui, R., Beauparlant, S., Vassiliev, I. R., Bryant, D. A., Jones, A. D., Golbeck, J. H., and Chitnis, P. R. (2000) Recruitment of a foreign quinone into the A_1 site of Photosystem I. I. Genetic and physiological characterization of phylloquinone biosynthetic pathway mutants in *Synechocystis* sp. PCC 6803. *J Biol Chem* **275**, 8523-8530
11. Semenov, A. Y., Vassiliev, I. R., van der Est, A., Mamedov, M. D., Zybailov, B., Shen, G., Stehlik, D., Diner, B. A., Chitnis, P. R., and Golbeck, J. H. (2000) Recruitment of a foreign quinone into the A_1 site of Photosystem I. Altered kinetics of electron transfer in phylloquinone biosynthetic pathway mutants studied by time-resolved optical, EPR, and electrometric techniques. *J Biol Chem* **275**, 23429-23438
12. Zybailov, B., van der Est, A., Zech, S. G., Teutloff, C., Johnson, T. W., Shen, G., Bittl, R., Stehlik, D., Chitnis, P. R., and Golbeck, J. H. (2000) Recruitment of a foreign quinone into the A_1 site of Photosystem I. II. Structural and functional characterization of

phylloquinone biosynthetic pathway mutants by electron paramagnetic resonance and electron-nuclear double resonance spectroscopy. *J Biol Chem* **275**, 8531-8539

13. Johnson, T. W., Zybailov, B., Jones, A. D., Bittl, R., Zech, S., Stehlik, D., Golbeck, J. H., and Chitnis, P. (2001) Recruitment of a foreign quinone into the A_1 site of Photosystem I. *In vivo* replacement of plastoquinone-9 by media-supplemented naphthoquinones in phylloquinone biosynthetic pathway mutants of *Synechocystis* sp. PCC 6803. *J Biol Chem* **276**, 31512-31521
14. Johnson, W. T., Naithani, S., Stewart, C., Zybailov, B., Daniel Jones, A., Golbeck, J. H., and Chitnis, P. R. (2003) The *menD* and *menE* homologs code for 2-succinyl-6-hydroxyl-2,4-cyclohexadiene-1-carboxylate synthase and O-succinylbenzoic acid-CoA synthase in the phylloquinone biosynthetic pathway of *Synechocystis* sp. PCC 6803. *Biochim Biophys Acta* **1557**, 67-76.
15. Lubner, C. E., Applegate, A. M., Knorzer, P., Ganago, A., Bryant, D. A., Happe, T., and Golbeck, J. H. (2011) Solar hydrogen-producing bionanodevice outperforms natural photosynthesis. *Proc Natl Acad Sci U S A* **108**, 20988-20991